

Hyperspectrally Compressed Ultrafast Photography

Chengshuai Yang,[‡] Fengyan Cao,[‡] Dalong Qi^{⑥,*}, Yilin He, Pengpeng Ding, Jiali Yao,
Tianqing Jia, Zhenrong Sun, and Shian Zhang^{⑥,†}

*State Key Laboratory of Precision Spectroscopy, School of Physics and Electronics Science,
East China Normal University, Shanghai 200062, China*



(Received 26 August 2019; published 16 January 2020)

The spatial, temporal, and spectral information in optical imaging play a crucial role in exploring the unknown world and unencrypting natural mysteries. However, the existing optical imaging techniques can only acquire the spatiotemporal or spatirospectral information of the object with the single-shot method. Here, we develop a hyperspectrally compressed ultrafast photography (HCUP) that can simultaneously record the spatial, temporal, and spectral information of the object. In our HCUP, the spatial resolution is 1.26 lp/mm in the horizontal direction and 1.41 lp/mm in the vertical direction, the temporal frame interval is 2 ps, and the spectral frame interval is 1.72 nm. Moreover, HCUP operates with receive-only and single-shot modes, and therefore it overcomes the technical limitation of active illumination and can measure the nonrepetitive or irreversible transient events. Using our HCUP, we successfully measure the spatiotemporal-spatiospectral intensity evolution of the chirped picosecond laser pulse and the photoluminescence dynamics. This Letter extends the optical imaging from three- to four-dimensional information, which has an important scientific significance in both fundamental research and applied science.

DOI: 10.1103/PhysRevLett.124.023902

In scientific research, it is very important to obtain the spatial structure, temporal evolution, and spectral composition of the object in order to better understand the natural phenomena. As a direct observation method, the optical imaging technique provides a powerful tool to explore the mysterious nature and unknown world due to its unique capability in the spatial, temporal, and spectral resolutions. However, the existing optical imaging methods can only obtain the spatiotemporal or spatirospectral information with the single-shot method, which greatly limits the information extraction of the object. For example, the ultrafast imaging techniques, including compressed ultrafast photography (CUP) [1–6], compressed ultrafast spectral-temporal (CUST) photography [7], and sequentially timed all-optical mapping photography (STAMP) [8], can only acquire the spatial and temporal information of the object. Both CUST photography and STAMP seem to be able to obtain the spectral information, but it is the spectrum of the illuminating light (i.e., the chirped femtosecond laser), not the spectrum emitted from the object, such as the fluorescence. Moreover, the spectral and temporal information in CUST photography and STAMP are coupled, and the spectral response of the object is usually neglected. However, the spectral imaging techniques, such as hyperspectral imaging [9–11] and coded aperture snapshot spectral imager [12–17], can only obtain the spatial and spectral information of the object.

To break the technical limitation of previous optical imaging methods in the detection dimension, here we develop a hyperspectrally compressed ultrafast photography

(HCUP) with the single-shot method, which has the ability to measure the object in all the spatial, temporal, and spectral dimensions. In our method, we transform the temporal and spectral information into the spatial dimension, and finally recover them by a computational imaging method based on compressed sensing algorithms [18–23]. In our HCUP, the spatial resolution is 1.26 lp/mm in the horizontal direction and 1.41 lp/mm in the vertical direction, and the temporal and spectral frame intervals can be up to 2 ps and 1.72 nm, respectively. To verify the HCUP's advantage, we successfully demonstrate the spatiotemporal-spatiospectral intensity evolution of the chirped picosecond laser pulse and the photoluminescence dynamics.

The HCUP principle is shown in Fig. 1(a). Here, the scene (i.e., object) involves the spatial, temporal, and spectral four-dimensional (4D) information, labeled with $I(x, y, t, \lambda)$. First, the scene is spatially encoded in the intensity by the random codes. Then, the encoded scene is horizontally deflected in the spectral domain, while is vertically deflected in the time domain. Finally, the encoded and deflected scene is measured by an array detector, labeled with $E(x', y')$. Mathematically, this imaging process can be described by an encoding operator \mathbf{C} , a spectral operator \mathbf{S} , a temporal operator \mathbf{T} , and a multiplexed operator \mathbf{M} . Thus, the measured image $E(x', y')$ can be formulated as

$$E(x', y') = \mathbf{MTSCI}(x, y, t, \lambda). \quad (1)$$

To recover the 4D scene $I(x, y, t, \lambda)$ from the two-dimensional (2D) image $E(x', y')$, it needs to solve the

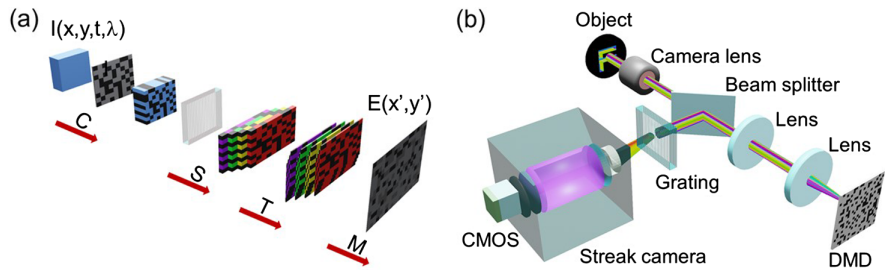


FIG. 1. HCUP principle and configuration. (a) HCUP principle. $I(x, y, t, \lambda)$ original scene: measurement image $E(x', y')$, encoding operator C , spectral operator S , temporal operator T , multiplexed operator M . (b) HCUP system configuration.

inverse problem of Eq. (1). One method is to calculate the minimal value of the following object function, and is given by

$$\hat{I} = \arg \min_I \left\{ \Phi_{TV}[I(x, y, t, \lambda)] - \Gamma[E(x', y') - \mathbf{MTSCI}(x, y, t, \lambda)] + \frac{Q}{2} \|E(x', y') - \mathbf{MTSCI}(x, y, t, \lambda)\|_2^2 \right\}, \quad (2)$$

where $\Phi_{TV}(\cdot)$ is the total variation (TV) regularizer, Γ is the Lagrange multiplier vector, Q is the penalty parameter, and $\|\cdot\|_2$ represents the l_2 norm. Here, we employ an augmented Lagrangian (AL) algorithm based on compressed sensing to solve Eq. (2) [18–20]. In the image reconstruction, the AL algorithm imposes the limitation that the scene is sparse in the TV domain.

The HCUP system configuration is given in Fig. 1(b). The object is imaged via a camera lens and a $4f$ imaging system consisting of two lenses. On the image plane, a

digital micromirror device (DMD) (Texas Instruments, DLP LightCrafter) is used to encode the scene in the spatial domain. Through the collection of the same $4f$ imaging system and the reflection of a beam splitter, the encoded scene is horizontally deflected in the spectral domain by a grating and then is further vertically deflected in the time domain by a streak camera (Hamamatsu, C7700). Finally, a complementary metal oxide semiconductor (CMOS) (Hamamatsu, ORCA-flash4.0) is employed to detect the encoded and deflected scene.

In our HCUP, the spectral frame interval is 1.72 nm, which is determined by the grating groove, and the temporal frame interval is 2 ps, which is limited by the deflection velocity of the streak camera. However, the spatial resolution depends on the performance of the whole optical imaging system. To characterize the spatial resolution, we use HCUP to image a resolution test chart, as shown in Fig. 2(a). In order to involve the temporal and spectral information, the resolution test chart is illuminated by two time-delayed femtosecond laser pulses. Here, the laser pulse width is about 50 fs, the central wavelength is 800 nm, and the time delay is set to be 32 ps.

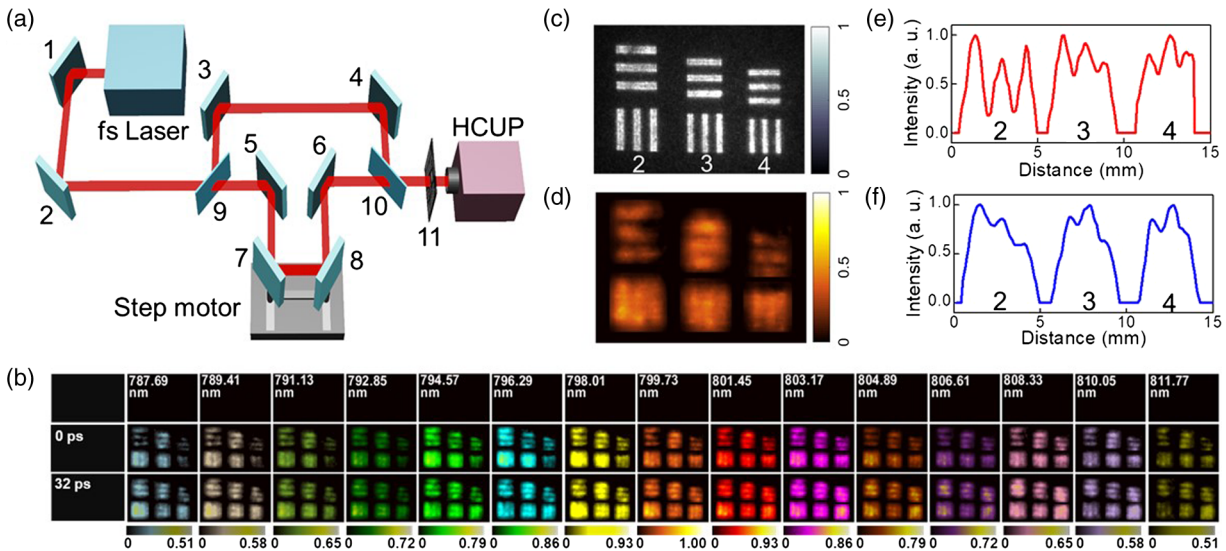


FIG. 2. Characterizing spatial resolution. (a) Experimental setup: (1–8) mirror, (9) and (10) beam splitter, (11) resolution test chart. (b) Reconstructed images of elements 2–4 in group 0 of test resolution target. (c),(d) Measured static image of test resolution target from external CCD and selected dynamic image from (b). (e),(f) Integrated intensities for horizontal and vertical lines in (d).

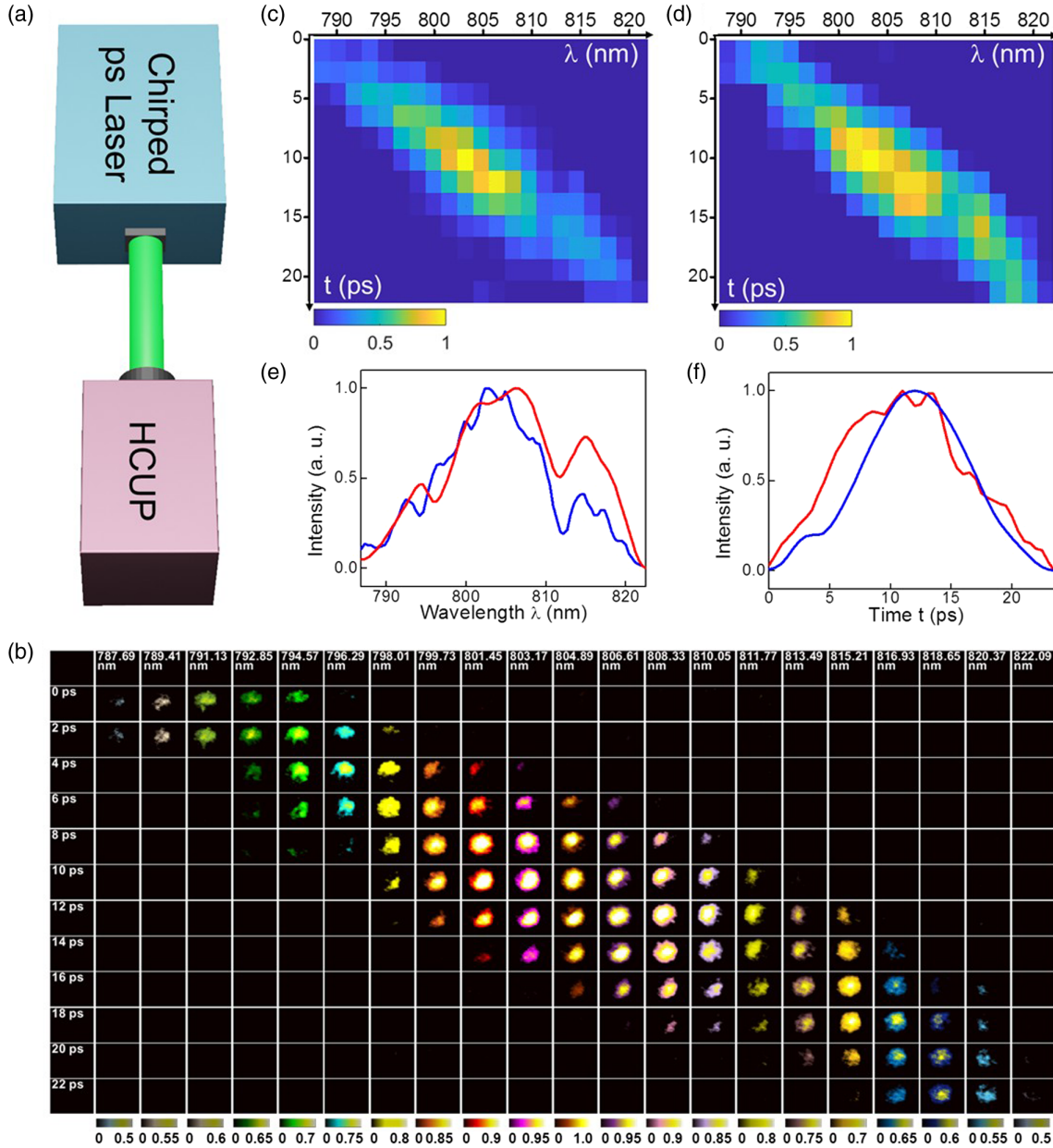


FIG. 3. Imaging chirped picosecond laser pulse. (a) Experimental design. (b) Reconstructed images. (c),(d) Time-resolved spectroscopies calculated from (b) and directly measured by the streak camera, respectively. (e),(f) Laser spectra and pulse durations calculated from (c) (red lines) and (d) (blue lines).

The static image of the resolution test chart without the deflections of the grating and streak camera is shown in Fig. 2(c). The dynamical images by our 4D image reconstruction are given in Fig. 2(b). Obviously, the spatial, temporal, and spectral information can be well recorded by HCUP. Compared with the static image, the dynamic images are a little blurred due to various operations on the scene, including encoding, deflection, superposition, and reconstruction. To more clearly demonstrate the image reconstruction quality, the reconstructed image with the time of 0 ps and the wavelength of 799.73 nm is selected, as shown in Fig. 2(d). Meanwhile, the intensities in these

elements with the horizontal (vertical) lines are integrated along the horizontal (vertical) direction, as shown in Figs. 2(e) and 2(f), respectively. In elements 2 and 3, both the horizontal and vertical lines are clearly distinguished. In element 4, the horizontal lines can still be distinguished, but the vertical lines cannot. For the smaller elements in the resolution test chart, both the horizontal and vertical lines are completely indistinguishable (not shown here). The spatial resolution of the horizontal (vertical) direction is characterized by the distinguishable ability of the vertical (horizontal) lines. In element 3, the linewidth is $396.85 \mu\text{m}$, and thus the spatial resolution in the horizontal direction can be

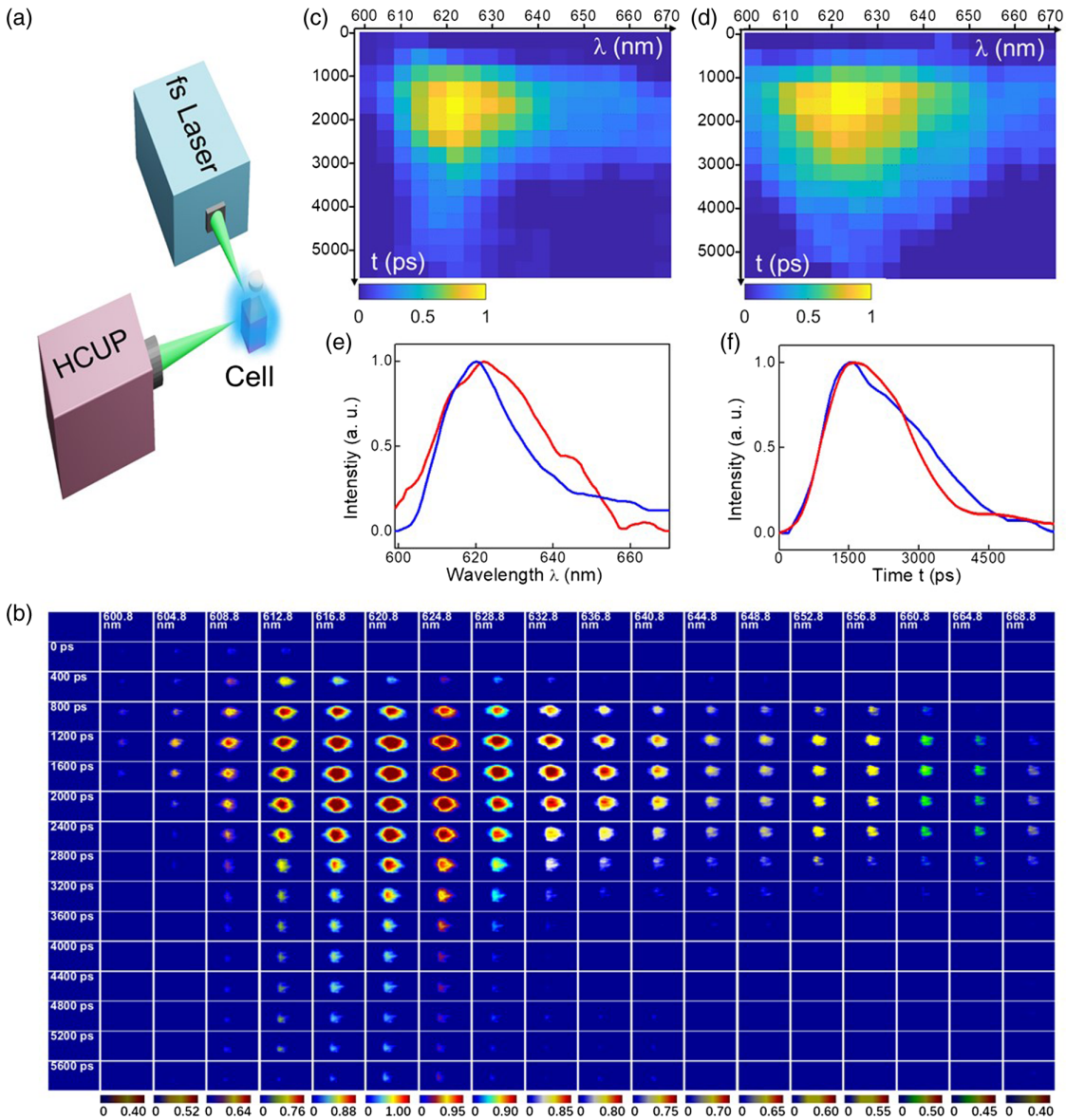


FIG. 4. Capturing photoluminescence dynamics. (a) Experimental arrangement. (b) Reconstructed images. (c),(d) Time-resolved spectroscopies calculated from (b) and directly measured by a streak camera, respectively. (e),(f) Fluorescence spectra and luminescence dynamics calculated from (c) (red lines) and (d) (blue lines).

determined as 1.26 lp/mm. In element 4, the linewidth is 353.55 μm , and the spatial resolution in the vertical direction is calculated to be 1.41 lp/mm.

The spatial, temporal, and spectral measurement of the ultrashort laser pulse is of great significance in characterizing the performance of the laser device and exploring the interaction of the laser and matter. Here, we use HCUP to measure the spatiotemporal-spatiospectral intensity evolution of a chirped picosecond laser pulse, and the experimental design is shown in Fig. 3(a). The chirped picosecond laser pulse is obtained by stretching an 80 fs laser pulse with a pulse stretcher. In this experiment, the chirped picosecond laser pulse width is about 10 ps, and the laser spectral bandwidth is about 28 nm with the central

wavelength at 800 nm. The reconstructed images at each temporal and spectral frame interval are presented in Fig. 3(b). As can be seen, the spatial distribution of the laser pulse at each reconstructed image can be clearly observed, and both the temporal and spectral intensity evolution behaviors can be well demonstrated. More importantly, the laser pulse appearance is almost linearly delayed with the increase in the laser wavelength, which is consistent with the characteristics of the chirped laser pulse. In order to further verify the accuracy of our experimental measurement, especially for the temporal and spectral information, we measure the time-resolved spectrum of the chirped picosecond laser pulse using the traditional method with the streak camera, as shown in Fig. 3(d). We

also calculate the time-resolved spectrum from Fig. 3(b) by integrating the intensity in each image, as shown in Fig. 3(c). For intuitive comparison, we extract the laser spectra and pulse durations from Figs. 3(c) and 3(d), as shown in Figs. 3(e) and 3(f), respectively. By comparing the experimental results of the two measurement methods, our method is consistent with the traditional method in recording the temporal and spectral information. Compared to previous CUP techniques that can only record the spatial and temporal information of the ultrashort laser pulse [24], here HCUP can simultaneously get all of the spectral information, which demonstrates a stronger detection capability.

As shown in Fig. 1, HCUP is a passive (or receive-only) optical imaging, which overcomes the technical limitation of active illumination. Therefore, an important application of HCUP is the luminescence dynamics measurement. Here, we capture the femtosecond laser-induced luminescence process in spatial, temporal, and spectral dimensions using HCUP, and the experiment arrangement is shown in Fig. 4(a). In this experiment, the rhodamine B dissolved in absolute ethyl alcohol is excited by a femtosecond laser with a pulse width of 50 fs and central wavelength of 800 nm, and the laser-induced fluorescence signal is measured by HCUP in the perpendicular direction of the laser propagation. The images at each temporal and spectral frame interval are reconstructed, as shown in Fig. 4(b). As expected, the spatiotemporal-spatiospectral intensity evolution behavior in the photoluminescence process can be clearly observed. Similarly, the time-resolved spectrum of the fluorescence signal is also measured by the streak camera for validating our experimental results, as shown in Fig. 4(d). Meanwhile, the time-resolved spectrum is also extracted from Fig. 4(b) for comparison, as shown in Fig. 4(c). Furthermore, the fluorescence spectra and luminescence dynamics are further extracted from Figs. 4(c) and 4(d), as shown in Figs. 4(e) and 4(f), respectively. By comparison, the experimental results by the two measurement methods are in good agreement. In previous multicolor CUP [1], the spectral components of the object are separated by a dichroic splitting strategy, and therefore only the sectional spectral information can be extracted. Unlike multicolor CUP, our HCUP is able to obtain the continuous spectral information.

In conclusion, we have reported a single-shot, receive-only, and 4D optical imaging technique, namely, HCUP. Compared to the existing optical imaging techniques that can only acquire spatial and temporal (or spectral) information with the single-shot method, HCUP can simultaneously record the spatial, temporal, and spectral information of the object. In our HCUP, the spatial resolutions in the horizontal and vertical directions are, respectively, 1.26 and 1.41 lp/mm, the temporal frame interval is 2 ps, and the spectral frame interval is 1.72 nm. Based on our HCUP, we realized the spatiotemporal-spatiospectral four-dimensional optical imaging of the chirped picosecond laser pulse and the

photoluminescence dynamics. In future studies, HCUP can be coupled to a variety of imaging modalities, involving microscopes and telescopes, which enable recording the object at the spatial scales from cellular organelles to galaxies. Considering the powerful function of HCUP in optical imaging, it will open a new route in related application areas.

This work was partially supported by the National Natural Science Foundation of China (Grants No. 91850202, No. 11774094, No. 11727810, No. 11804097, and No. 61720106009), the Science and Technology Commission of Shanghai Municipality (Grants No. 19560710300 and No. 17ZR146900), and the China Postdoctoral Science Foundation (Grant No. 2018M641958).

^{*}Corresponding author.

dlqi@lps.ecnu.edu.cn

[†]Corresponding author.

sazhang@phy.ecnu.edu.cn

[#]These authors contributed equally to this work.

- [1] L. Gao, J. Liang, C. Li, and L. V. Wang, Single-shot compressed ultrafast photography at one hundred billion frames per second, *Nature (London)* **516**, 74 (2014).
- [2] J. Liang, C. Ma, L. Zhu, Y. Chen, L. Gao, and L. V. Wang, Single-shot real-time video recording of a photonic Mach cone induced by a scattered light pulse, *Sci. Adv.* **3**, e1601814 (2017).
- [3] L. Zhu, Y. Chen, J. Liang, Q. Xu, L. Gao, C. Ma, and L. V. Wang, Space- and intensity-constrained reconstruction for compressed ultrafast photography, *Optica* **3**, 694 (2016).
- [4] C. Yang, D. Qi, X. Wang, F. Cao, Y. He, W. Wen, T. Jia, J. Tian, Z. Sun, L. Gao, S. Zhang, and L. V. Wang, Optimizing codes for compressed ultrafast photography by the genetic algorithm, *Optica* **5**, 147 (2018).
- [5] J. Liang, L. Zhu, L. Zhu, and L. V. Wang, Single-shot real-time femtosecond imaging of temporal focusing, *Light Sci. Appl.* **7**, 42 (2018).
- [6] C. Yang, D. Qi, J. W. Liang, X. Wang, F. Cao, Y. He, X. Ouyang, B. Zhu, W. Wen, T. Jia, J. Tian, L. Gao, Z. Sun, S. Zhang, and L. V. Wang, Compressed ultrafast photography multi-encoding imaging, *Laser Phys. Lett.* **15**, 116202 (2018).
- [7] Y. Lu, T. T. Wong, F. Chen, and L. Wang, Compressed Ultrafast Spectral-Temporal Photography, *Phys. Rev. Lett.* **122**, 193904 (2019).
- [8] K. Nakagawa, A. Iwasaki, Y. Oishi, R. Horisaki, A. Tsukamoto, A. Nakamura, and F. Kannari, Sequentially timed all-optical mapping photography (STAMP), *Nat. Photonics* **8**, 695 (2014).
- [9] L. Gao, R. T. Kester, and T. S. Tkaczyk, Compact image slicing spectrometer (ISS) for hyperspectral fluorescence microscopy, *Opt. Express* **17**, 12293 (2009).
- [10] S. Vivès and E. Prieto, Original image slicer designed for integral field spectroscopy with the near-infrared spectrograph for the James Webb Space Telescope, *Opt. Eng.* **45**, 093001 (2006).

- [11] F. Hénault, R. Bacon, R. Content, B. Lantz, F. Laurent, J. P. Lemonnier, and S. L. Morris, Slicing the universe at affordable cost: The quest for the MUSE image slicer, *Proc. SPIE Int. Soc. Opt. Photonics* **5249**, 134 (2004).
- [12] M. E. Gehm, R. John, D. J. Brady, R. M. Willett, and T. J. Schulz, Single-shot compressive spectral imaging with a dual-disperser architecture, *Opt. Express* **15**, 14013 (2007).
- [13] A. Wagadarikar, R. John, R. Willett, and D. Brady, Single disperser design for coded aperture snapshot spectral imaging, *Appl. Opt.* **47**, B44 (2008).
- [14] D. Kittle, K. Choi, A. Wagadarikar, and D. J. Brady, Multiframe image estimation for coded aperture snapshot spectral imagers, *Appl. Opt.* **49**, 6824 (2010).
- [15] G. R. Arce, D. J. Brady, L. Carin, H. Arguello, and D. S. Kittle, Compressive coded aperture spectral imaging: An introduction, *IEEE Signal Process. Mag.* **31**, 105 (2013).
- [16] S. T. McCain, M. E. Gehm, Y. Wang, N. P. Pitsianis, and D. J. Brady, Coded aperture Raman spectroscopy for quantitative measurements of ethanol in a tissue phantom, *Appl. Spectrosc.* **60**, 663 (2006).
- [17] C. Fernandez, B. D. Guenther, M. E. Gehm, D. J. Brady, and M. E. Sullivan, Longwave infrared (LWIR) coded aperture dispersive spectrometer, *Opt. Express* **15**, 5742 (2007).
- [18] C. Yang, D. Qi, F. Cao, Y. He, X. Wang, W. Wen, J. Tian, J. Tian, Z. Sun, and S. Zhang, Improving the image reconstruction quality of compressed ultrafast photography via an augmented Lagrangian algorithm, *J. Optics* **21**, 035703 (2019).
- [19] M. V. Afonso, J. M. Bioucas-Dias, and M. A. Figueiredo, An augmented Lagrangian approach to the constrained optimization formulation of imaging inverse problems, *IEEE Trans. Image Process.* **20**, 681 (2011).
- [20] C. Li, An efficient algorithm for total variation regularization with applications to the single pixel camera, and compressive sensing, Master Thesis, Rice University, 2009.
- [21] E. Candes and T. Tao, Near optimal signal recovery from random projections: Universal encoding strategies?, *IEEE Trans. Inf. Theory* **52**, 5406 (2006).
- [22] E. J. Candès, J. K. Romberg, and T. Tao, Stable signal recovery from incomplete and inaccurate measurements, *Commun. Pure Appl. Math.* **59**, 1207 (2006).
- [23] R. M. Willett, R. F. Marcia, and J. M. Nichols, Compressed sensing for practical optical imaging systems: A tutorial, *Opt. Eng.* **50**, 072601 (2011).
- [24] F. Cao, C. Yang, D. Qi, J. Yao, Y. He, X. Wang, and S. Zhang, Single-shot spatiotemporal intensity measurement of picosecond laser pulses with compressed ultrafast photography, *Opt. Lasers Eng.* **116**, 89 (2019).